Supplement to "Practical analytical solutions for benchmarking of 2-D and 3-D geodynamic Stokes problems with variable viscosity"

1 Example problems and numerical convergence tests

The scheme of algorithm testing is conventional. We have obtained particular solutions of the Stokes and continuity equations for two types of viscosity variations. Let us choose a domain, e.g., a rectangle in 2D case. Calculate values of velocity and pressure given by our analytical solution and take this values as the boundary conditions. Then, due to the uniqueness theorem the solution of the boundary problem in the domain should coincide with our analytical solution. Let us compute the solution of the boundary problem by a numerical method. Comparison of the result with the exact analytical solution shows the quality of the numerical algorithm. In the present paper, we used standard 2D and 3D stress-conservative finite-differences on staggered regularly spaced grid for obtaining numerical solutions (Gerya et al., 2010). Respective MatLab programs for 2D and 3D cases are provided as supplements to this paper.

1.1 2D example

1.1.1 Linearly varying viscosity

Consider a simple example of such flow in a rectangle $0 \le x \le x_{size}, 0 \le y \le y_{size}$. We assume that $\eta = ax + by + c$. We will mark the exact solution obtained in Section 2 as $v_{x,a}, v_{y,a}, P_a$. It is the solution of the boundary problem in the rectangle Ω with the following conditions at the boundary $\partial\Omega = \{x = 0, x = x_{size}, y = 0, y = y_{size}\}$:

$$v_y|_{\partial\Omega} = v_{y,a}, \quad v_x|_{\partial\Omega} = v_{x,a}.$$

Let us compute the velocity and pressure with using of finite-difference scheme. The corresponding solution is marked as $v_{x,n}, v_{y,n}, P_n$. The deviation of these values from the exact solution $(v_{x,n} - v_{x,a}, v_{y,n} - v_{y,a}, P_n - P_a)$ is related with the error of the numerical scheme We calculate the relative errors of three types: L_∞, L_1, L_2 for different viscosity contrasts , i.e. different values of the coefficients a, b. We test the program Stokes2D-variable-viscosity1 from [?]. The results are presented at Fig. 1 - 6. Namely, figures 1-3 correspond to low viscosity contrast, Figures 4-6 - to high viscosity contrast. Particularly, Fig. 1 and Fig. 4 show pressure and velocity components distributions. Fig. 2 and Fig. 4 characterizes the viscosity and the density distributions. Fig. 3 and Fig. 6 contain plots of relative errors via the grid resolutions in logarithmic scale. The viscosity contrast, i.e.

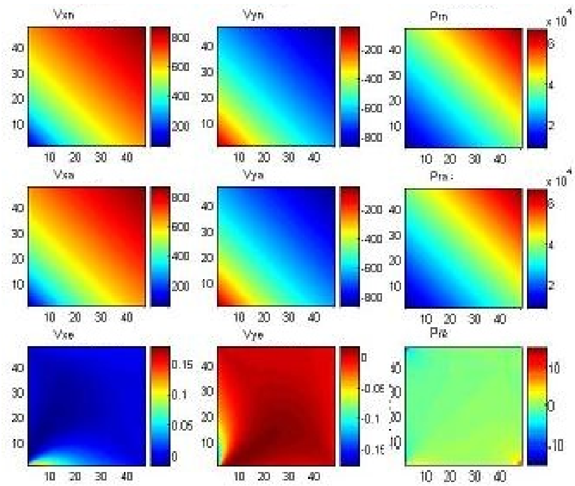

Figure 1: Distribution of v_x, v_y and P; 2D case, linearly varying viscosity, low viscosity contrast ($\eta_2 = \eta_3 = 5$). Here and in the following indices at the computed velocity components and pressure indicate analytical (a) and numerical (n) values and difference between them (e).

the values of the coefficients in the expression for the viscosity, is determined by given values of the viscosity at three rectangle corners. The value of the viscosity at the initial rectangle corner is 1, η_2, η_3 are the values of the viscosity at two adjacent corners. At all figures "n" means "numerical solution", "a" means "analytical solution" (benchmark).

For the case of linearly varying viscosity we made calculations for the following system parameters:

$$x_{size} = y_{size} = 1, G_x = 0, G_y = 10,$$

$$\eta_1 = 1, \beta_1 = 1, \beta_2 = 3 \times 10^3,$$

$$c = \eta_1, a = (\eta_3 - \eta_1)/x_{size}, b = (\eta_2 - \eta_1)/y_{size},$$

$$\rho = \beta_1(ax + by + c) + \beta_2.$$

One can see that there is rather high accuracy of the numerical approach. We observe the conventional situation - L_∞-error is the largest among the considered errors norms, and L_1-error and L_2-error are similar. The calculations show that one has good convergence of the numerical scheme for small viscosity contrast, but it is not so for high viscosity contrast (compare Fig. 3 and Fig. 6).

To describe in more details the dependence of the error on the viscosity contrast we fill tables with errors for different values of η_2, η_3 (see Appendix, tables 1-9).

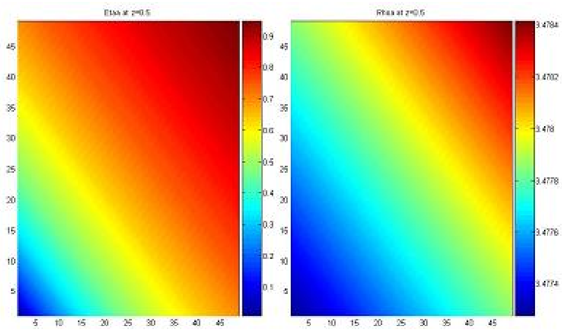

Figure 2: Distribution of viscosity η and density ρ; 2D case, linearly varying viscosity, low viscosity contrast ($\eta_2 = \eta_3 = 5$).

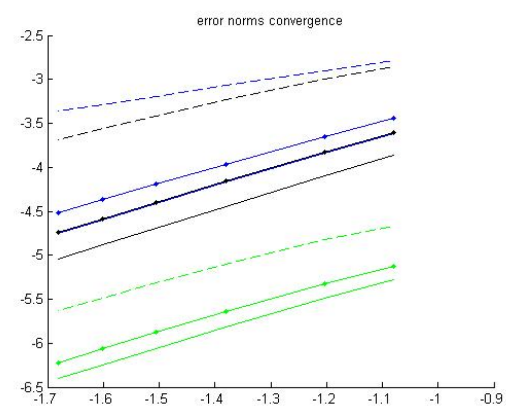

Figure 3: Logarithm of the relative error via logarithm of the grid step; 2D case, linearly varying viscosity, low viscosity contrast ($\eta_2 = \eta_3 = 5$); blue line - pressure, green - v_x, black - v_y; line - L_1-error, dashed line - L_∞-error, line with dots - L_2-error.

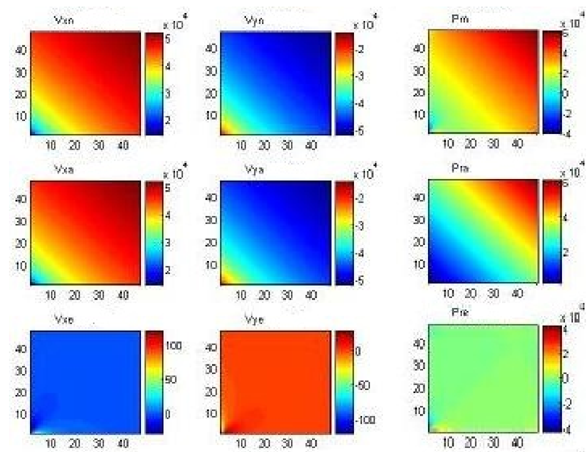

Figure 4: Distribution of v_x, v_y and P; 2D case, linearly varying viscosity, high viscosity contrast ($\eta_2 = \eta_3 = 100$).

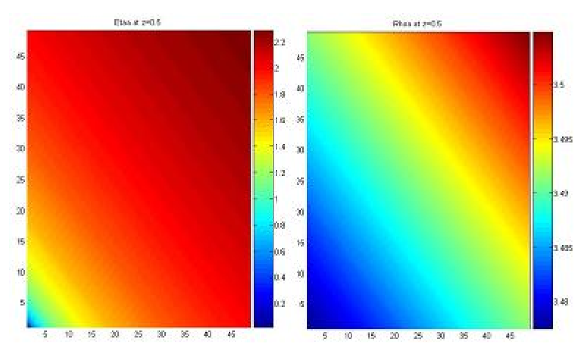

Figure 5: Distribution of viscosity η and density ρ; 2D case, linearly varying viscosity, high viscosity contrast ($\eta_2 = \eta_3 = 100$).

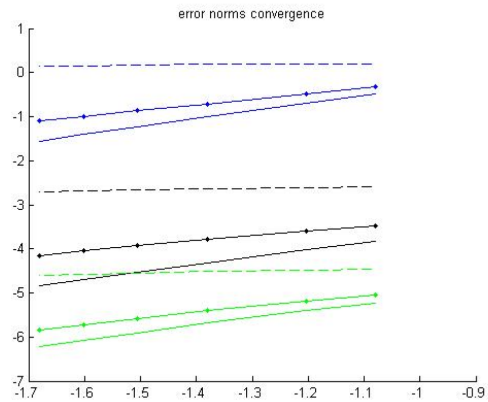

Figure 6: Logarithm of the relative error via logarithm of the grid step; 2D case, linearly varying viscosity, high viscosity contrast ($\eta_2 = \eta_3 = 100$); blue line - pressure, green - v_x, black - v_y; line - L_1-error, dashed line - L_∞-error, line with dots - L_2-error.

1.1.2 Exponentially varying viscosity

The case of exponentially varying viscosity is treated analogously. To have a possibility of comparison with the case of linearly varying viscosity we take the same system parameters (geometrical size, gravitational terms and the dependence of the density on the viscosity) with the same viscosity contrast (i.e. the values of the viscosity at the rectangle corners)

$$C = \eta_1, a = (\log(\eta_3) - \log(\eta_1))/x_{size},$$
$$b = (\log(\eta_2) - \log(\eta_1))/y_{size},$$
$$\eta = C \exp{(ax + by)},$$
$$\rho = \beta_1 \eta + \beta_2$$
$$x_{size} = y_{size} = 1,$$
$$G_x = 10, G_y = 10,$$
$$\eta_1 = 1, \beta_1 = 1, \beta_2 = 3 \times 10^3,$$

We deal with two cases (low and high viscosity contrasts). Figures 7-12 present the results. Namely, figures 7-9 correspond to the case of low viscosity contrast, figures 10-12 are related with the case of high viscosity contrast. There are some similarities with the previous case. Particularly, L_∞ error norm gives us the maximum relative error value among three considered error norms. We have small errors (see the velocity and pressure distributions, Fig. 7, Fig. 10). But

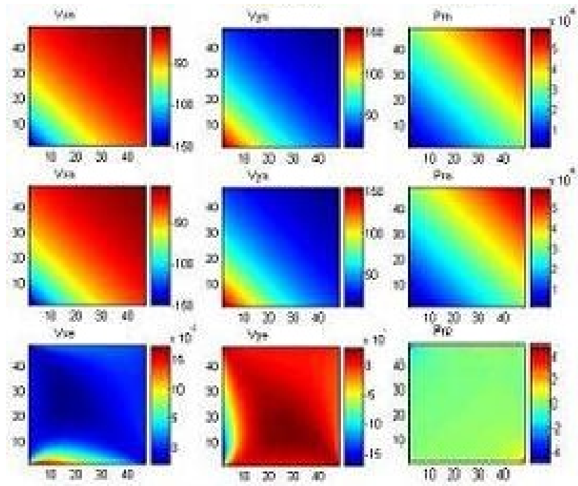

Figure 7: Distribution of v_x, v_y and P; 2D case, exponentially varying viscosity, low viscosity contrast ($\eta_2 = \eta_3 = 5$).

peculiarities are more interesting. Namely, the numerical scheme works essentially better for the case of exponentially varying viscosity than for linearly varying viscosity. We observe good convergence both for low and for high viscosity contrasts (compare Fig. 9, Fig. 12 and, correspondingly, Fig. 3, Fig. 6).

Dependence of the errors on the viscosity contrast for exponentially varying viscosity is presented in the tables 10-18 in Appendix.

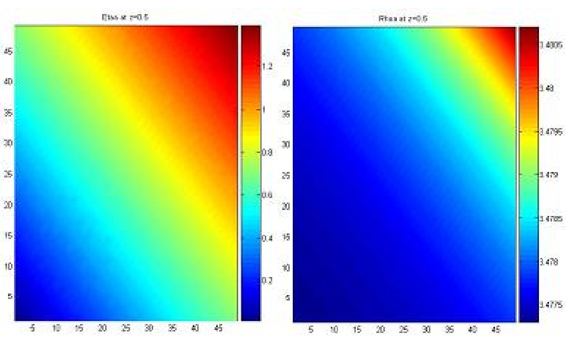

Figure 8: Distribution of viscosity η and density ρ; 2D case, exponentially varying viscosity, low viscosity contrast ($\eta_2 = \eta_3 = 5$).

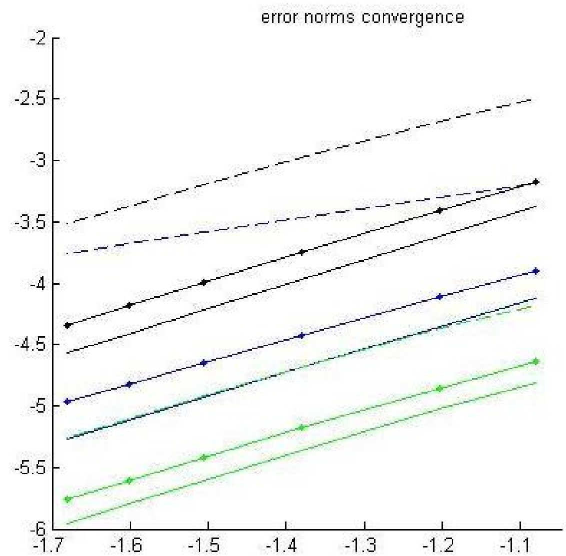

Figure 9: Logarithm of the relative error via logarithm of the grid step; 2D case, exponentially varying viscosity, low viscosity contrast ($\eta_2 = \eta_3 = 5$); blue line - pressure, green - v_x, black - v_y; line - L_1-error, dashed line - L_∞-error, line with dots - L_2-error.

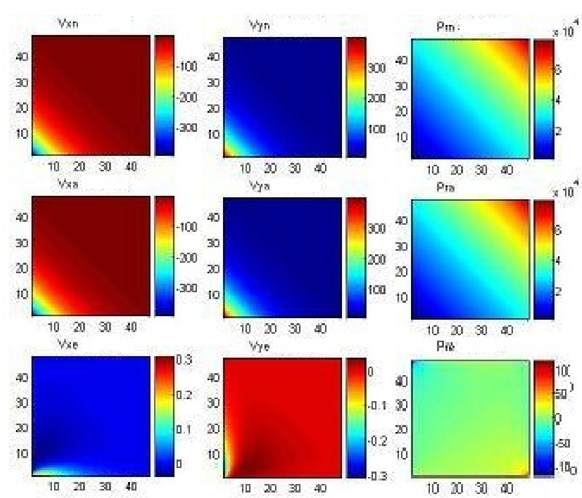

Figure 10: Distribution of v_x, v_y and P; 2D case, exponentially varying viscosity, high viscosity contrast ($\eta_2 = \eta_3 = 100$).

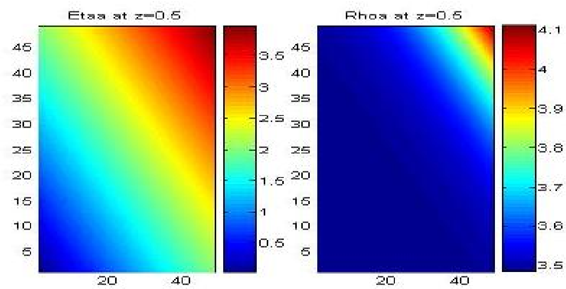

Figure 11: Distribution of viscosity η and density ρ; 2D case, exponentially varying viscosity, high viscosity contrast ($\eta_2 = \eta_3 = 100$).

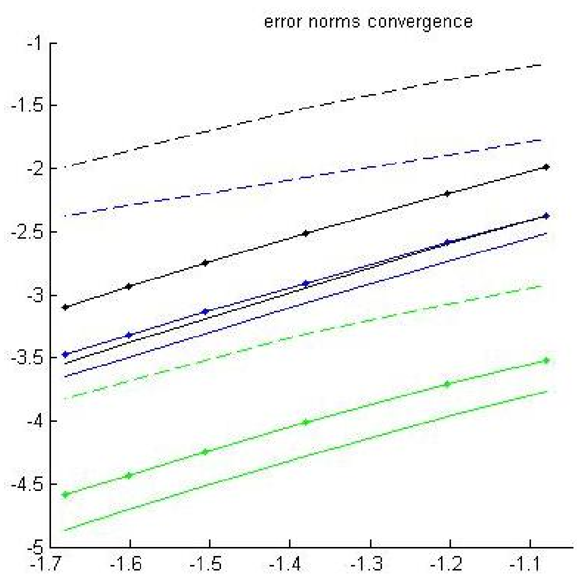

Figure 12: Logarithm of the relative error via logarithm of the grid step; 2D case, exponentially varying viscosity, high viscosity contrast ($\eta_2 = \eta_3 = 100$); blue line - pressure, green - v_x, black - v_y; line - L_1-error, dashed line - L_∞-error, line with dots - L_2-error.

1.2 3D example

One can note that benchmark solutions for 3D case are essentially more rare than for the corresponding 2D situation. It is remarkable that the suggested approach allows us to obtain such solutions for 3D Stokes and continuity equations. As earlier, we consider the cases of linearly and exponentially varying viscosity.

1.2.1 Linearly varying viscosity

The statement of the problem is absolutely analogous to the previous case. In 3D space we consider a parallelepiped Ω**:** $0 \leq x \leq x_{size}, 0 \leq y \leq y_{size}, 0 \leq z \leq z_{size}$. **We assume that** $\eta = ax + by + cz + e$. **We will mark the exact solution obtained in Section 3 as** $v_{x,a}, v_{y,a}, v_{z,a}, P_a$**. Due to the uniqueness theorem, it is the solution of the boundary problem in the parallelepiped** Ω **with the following conditions at the boundary** $\partial\Omega = \{x = 0, x = x_{size}, y = 0, y = y_{size}, z = 0, z = z_{size}\}$:

$$v_x|_{\partial\Omega} = v_{x,a}, v_y|_{\partial\Omega} = v_{y,a}, v_z|_{\partial\Omega} = v_{z,a}.$$

Let us compute the velocity and pressure with using of chosen finite-difference algorithm. The corresponding numerical solution is marked as $v_{x,n}, v_{y,n}, v_{z,n}, P_n$**. The deviation of these values from the exact solution** $(v_{x,n} - v_{x,a}, v_{y,n} - v_{y,a}, v_{z,n} - v_{z,a}, P_n - P_a)$ **is related with the error of the numerical scheme. As in 2D case, we consider three error norms:** L_∞, L_1, L_2**. We deal with cases of low and high viscosity contrasts. Coefficients** a, b, c, e **in the viscosity formula are determined through given viscosity values** $(\eta_1 = 1, \eta_2, \eta_3, \eta_4)$ **at four adjacent parallelepiped vertices. We choose the following system parameters:**

$$e = \eta_1, a = (\eta_3 - \eta_1)/x_{size},$$

$$b = (\eta_2 - \eta_1)/y_{size}, c = (\eta_4 - \eta_1)/z_{size}.$$

$$\eta = ax + by + cz + e,$$

$$\rho = \beta_1\eta + \beta_2$$

$$x_{size} = y_{size} = z_{size} = 1,$$

$$G_x = 10, G_y = 10, G_z = 0,$$

$$\eta_1 = 1, \beta_1 = 1, \beta_2 = 3 \times 10^3,$$

Results are presented at Fig. 13-20. Figures 13-16 correspond to the case of low viscosity contrast, figures 17-20 - to the case of high viscosity contrast. Figures 13, 14 and figures 17, 18 shows the velocity components and the pressure distribution for the central cross-section of the parallelepiped. The analytical and the numerical solutions and also the error (the solutions deviations) are shown. Fig. 15,

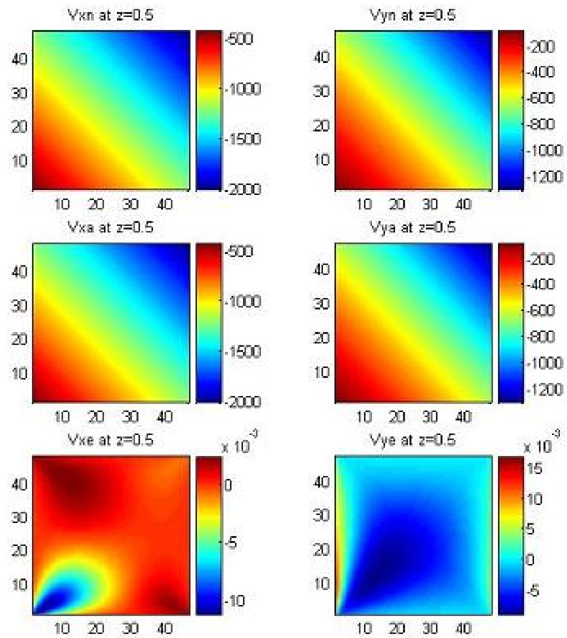

Figure 13: Distribution of v_x and v_y; 3D case, linearly varying viscosity, low viscosity contrast ($\eta_2 = \eta_3 = \eta_4 = 5$).

19 characterizes the distribution of the viscosity and the density for the same cross-section. In Fig. 16, 20 the errors for a sequence of grid resolution used to solve the equations numerically are provided. Positive slope of the curves shows the algorithm convergence. It should be mentioned that the numerical procedure for 3D case takes essentially greater time than in 2D case. Qualitatively, the results are similar to that for the corresponding 2D case. The numerical procedure works better for low viscosity contrast.

1.2.2 Exponentially varying viscosity

As in 2D case, we consider also exponentially varying viscosity. Consideration is absolutely parallel to that in the previous section. To have a possibility of comparison we take here the same system parameters. Naturally, the viscosity and, correspondingly, density distributions are now exponential. The system parameters are chosen by the following manner:

$$C = \eta_1, a = (\log(\eta_3) - \log(\eta_1))/x_{size},$$
$$b = (\log(\eta_2) - \log(\eta_1))/y_{size}, c = (\log(\eta_4) - \log(\eta_1))/z_{size}.$$

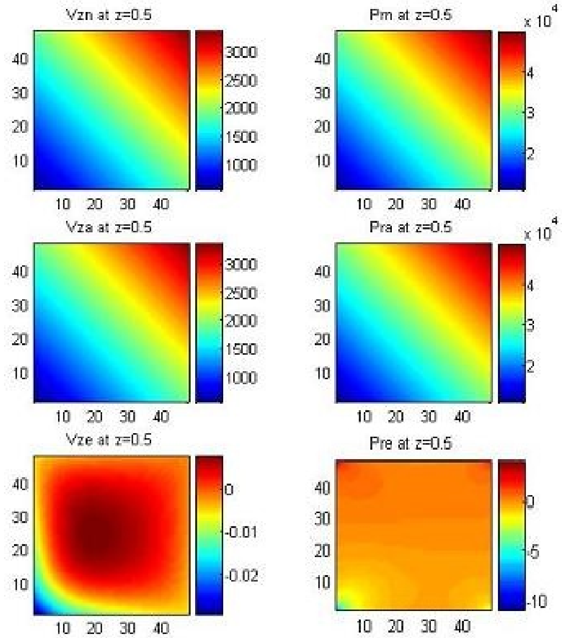

Figure 14: Distribution of v_z and P; 3D case, linearly varying viscosity, low viscosity contrast ($\eta_2 = \eta_3 = \eta_4 = 5$).

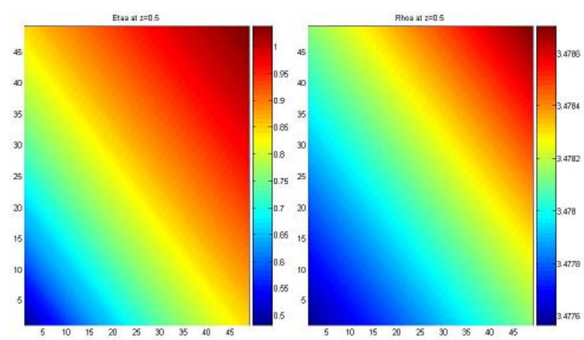

Figure 15: Distribution of viscosity η and density ρ; 3D case, linearly varying viscosity, low viscosity contrast ($\eta_2 = \eta_3 = \eta_4 = 5$).

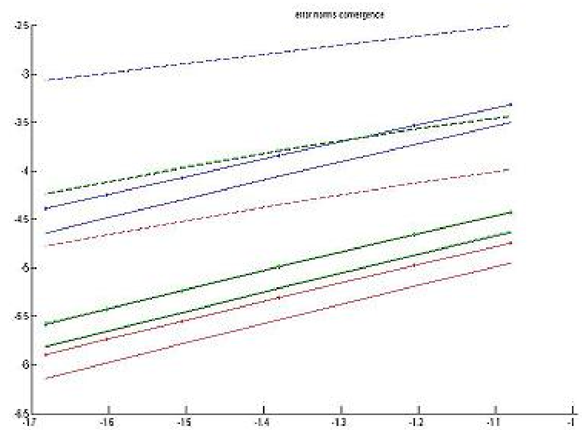

Figure 16: Logarithm of the relative error via logarithm of the grid step; 3D case, linearly varying viscosity, low viscosity contrast ($\eta_2 = \eta_3 = \eta_4 = 5$); blue line - pressure, red - v_x, black - v_y, green - v_z; line - L_1-error, dashed line - L_∞-error, line with dots - L_2-error.

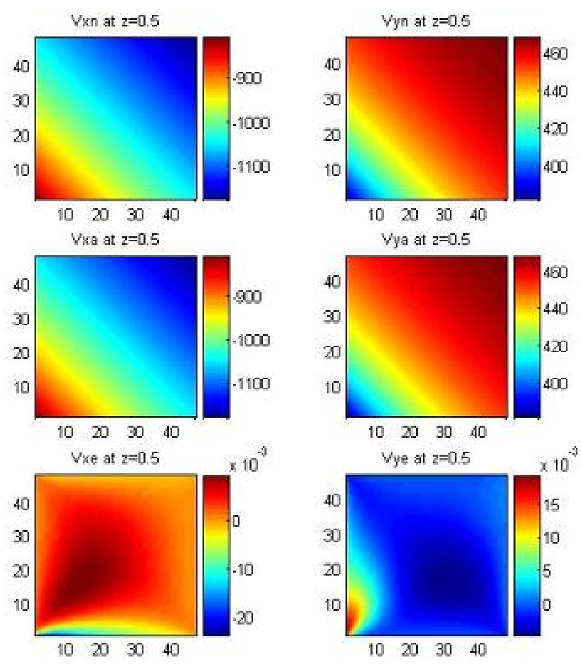

Figure 17: Distribution of v_x and v_y; 3D case, linearly varying viscosity, high viscosity contrast ($\eta_2 = \eta_3 = \eta_4 = 100$).

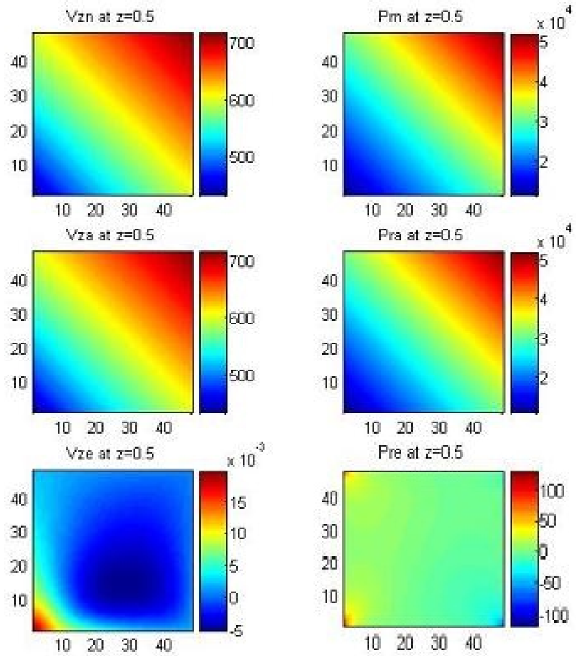

Figure 18: Distribution of v_z and P; 3D case, linearly varying viscosity, high viscosity contrast ($\eta_2 = \eta_3 = \eta_4 = 100$).

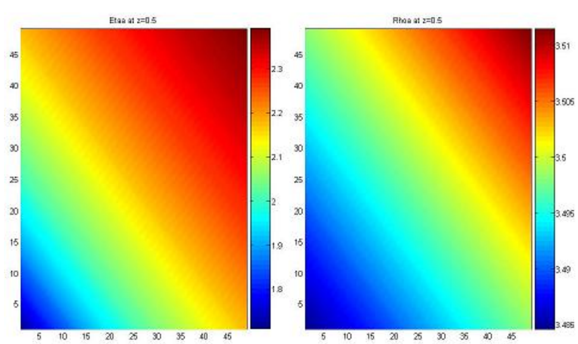

Figure 19: Distribution of viscosity η and density ρ; 3D case, linearly varying viscosity, high viscosity contrast ($\eta_2 = \eta_3 = \eta_4 = 100$).

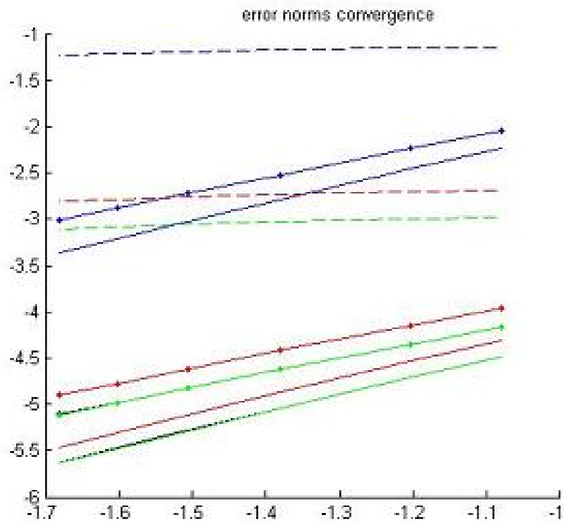

Figure 20: Logarithm of the relative error via logarithm of the grid step; 3D case, linearly varying viscosity, high viscosity contrast ($\eta_2 = \eta_3 = \eta_4 = 100$); blue line - pressure, red - v_x, black - v_y, green - v_z; line - L_1-error, dashed line - L_∞-error, line with dots - L_2-error.

$$\eta = C \exp{(ax + by + cz)},$$

$$\rho = \beta_1 \eta + \beta_2$$

$$x_{size} = y_{size} = z_{size} = 1,$$

$$G_x = 10, G_y = 10, G_z = 0,$$

$$\eta_1 = 1, \beta_1 = 1, \beta_2 = 3 \times 10^3,$$

The results are presented at Fig. 21-28. Figures 21-24 correspond to the case of low viscosity contrast, figures 25-28 - to the case of high viscosity contrast. It occurs that for exponentially varying viscosity the numerical algorithm works better than for linearly varying viscosity (compare the velocity and the pressure distributions and the corresponding errors at Fig. 21, 22, 25, 26 with Fig. 13, 14, 17, 18). It is in correlation with 2D case. The algorithm convergence, i.e. the dependence of the errors on the grid resolution is shown at Fig. 24, 28. One can see that "exponential" case gives us better convergence than the corresponding "linear" case.

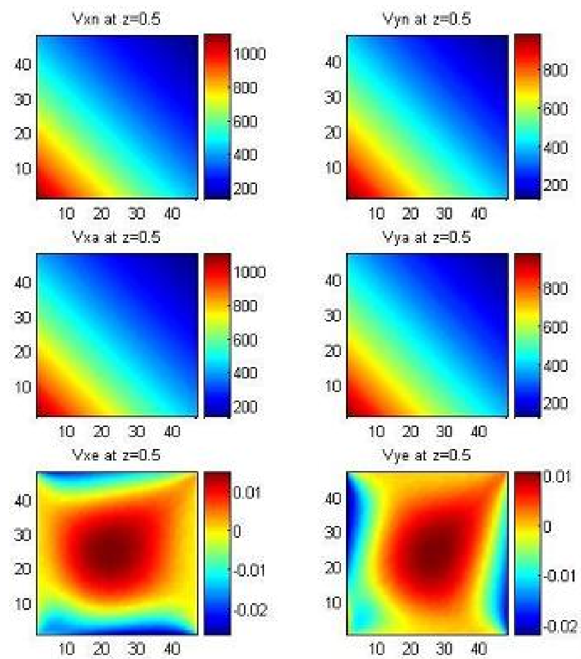

Figure 21: Distribution of v_x and v_y; 3D case, exponentially varying viscosity, low viscosity contrast ($\eta_2 = \eta_3 = \eta_4 = 5$).

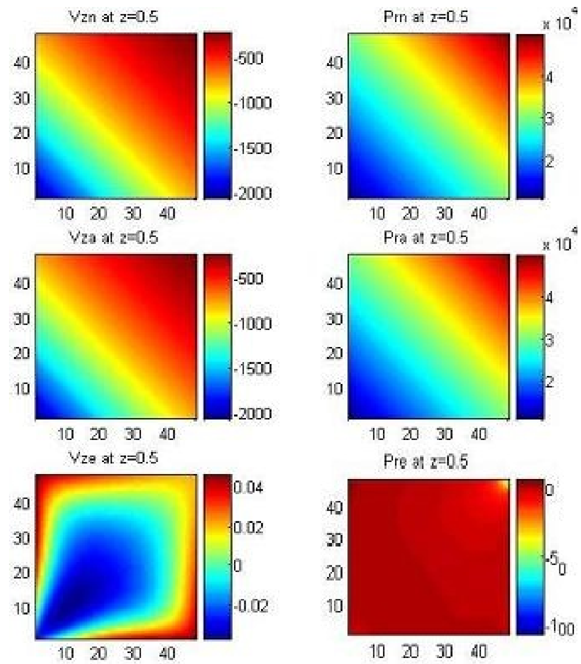

Figure 22: Distribution of v_z and P; 3D case, exponentially varying viscosity, low viscosity contrast ($\eta_2 = \eta_3 = \eta_4 = 5$).

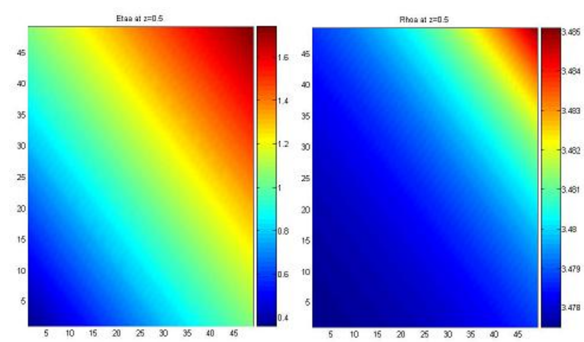

Figure 23: Distribution of viscosity η and density ρ; 3D case, exponentially varying viscosity, low viscosity contrast ($\eta_2 = \eta_3 = \eta_4 = 5$).

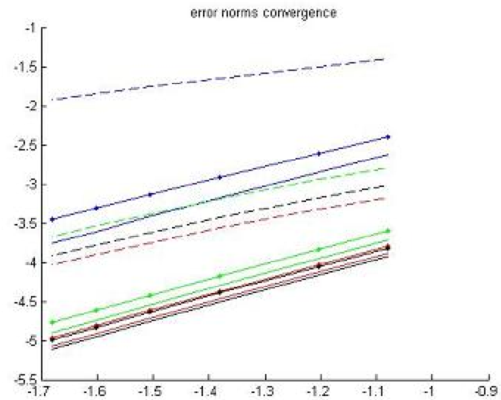

Figure 24: Logarithm of the relative error via logarithm of the grid step; 3D case, exponentially varying viscosity, low viscosity contrast ($\eta_2 = \eta_3 = \eta_4 = 5$); blue line - pressure, red - v_x, black - v_y, green - v_z; line - L_1-error, dashed line - L_∞-error, line with dots - L_2-error.

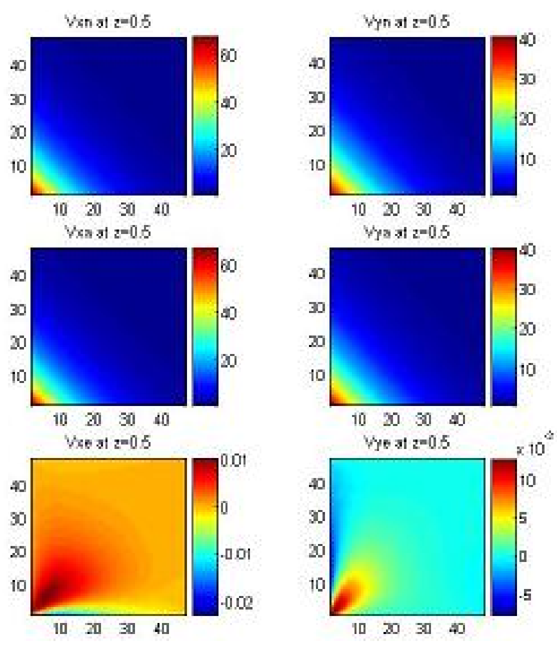

Figure 25: Distribution of v_x and v_y; 3D case, exponentially varying viscosity, high viscosity contrast ($\eta_2 = \eta_3 = \eta_4 = 100$).

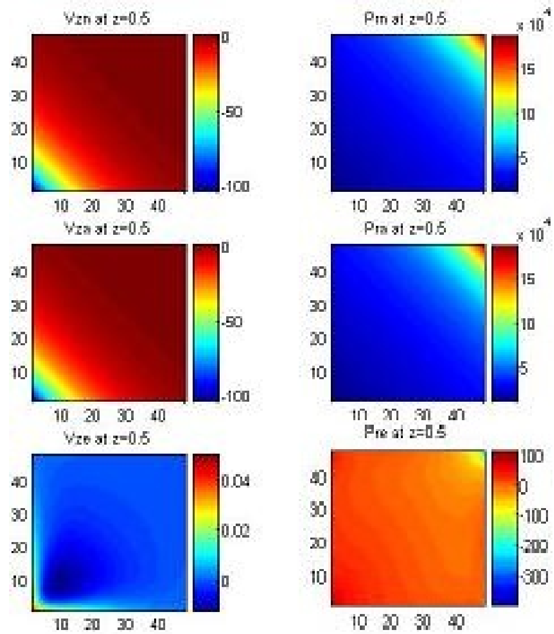

Figure 26: Distribution of v_z and P; 3D case, exponentially varying viscosity, high viscosity contrast ($\eta_2 = \eta_3 = \eta_4 = 100$).

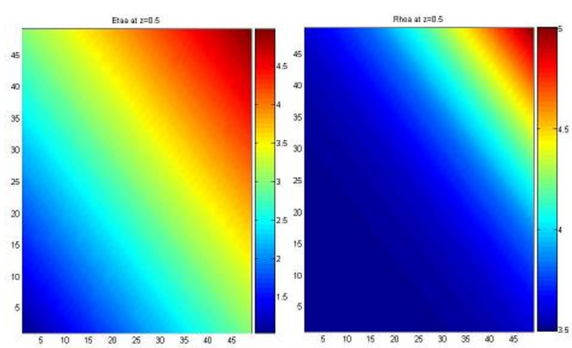

Figure 27: Distribution of viscosity η and exponentially varying viscosity, high viscosity contrast ($\eta_2 = \eta_3 = \eta_4 = 100$).

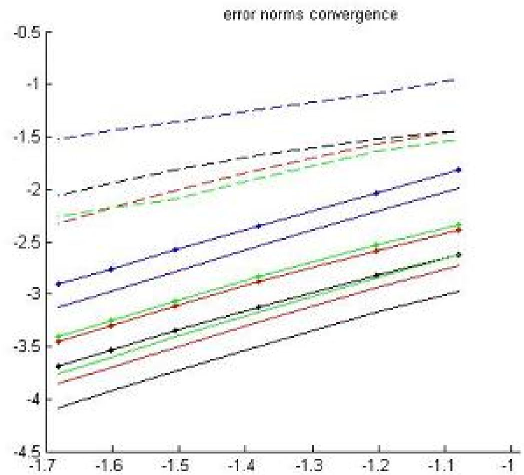

Figure 28: Logarithm of the relative error via logarithm of the grid step; 3D case, exponentially varying viscosity, high viscosity contrast ($\eta_2 = \eta_3 = \eta_4 = 100$); blue line - pressure, red - v_x, black - v_y, green - v_z; line - L_1-error, dashed line - L_∞-error, line with dots - L_2-error.

2 Error decreasing via the grid resolution decreasing

The dependence of the convergence on the viscosity contrast is shown in the following tables. Namely, the viscosities η_2, η_3 run through a set of values from 2 to 10000. For each pair of η_2, η_3 we perform the benchmarking procedure described above and obtain the curve describing the dependence of the logarithm of the error norm on the logarithm of the grid resolution. The tangent of the slope angle of this curve gives us an input of the table. Full set of tables is given in supplementary materials. Below, we show several examples of such tables.

2.1 Linearly varying viscosity

Tables A1–A9 contain log rates of error decreasing via the grid resolution decreasing (the curve slope at Figs. 3 and 6 in logarithmic scale) for different viscosity contrasts in the case of linearly varying viscosity. Calculations were made for the following system parame-

Table 1: Pressure; L_∞-error.

η_2 / η_3	2	5	20	100	300	1000	10 000
2	0.89	0.97	0.81	0.46	0.11	−0.19	−0.40
5	0.96	0.93	0.89	0.77	0.14	−0.14	−0.39
20	0.83	0.89	0.86	0.77	0.73	−0.06	−0.33
100	0.80	0.79	0.77	0.83	0.77	0.46	−0.21
300	0.76	0.76	0.77	0.79	0.83	0.79	−0.11
1000	0.49	0.61	0.73	0.77	0.77	0.83	0.14
10 000	−0.40	−0.39	−0.33	−0.21	0.13	0.41	0.80

Table 2: Pressure; L_1-error.

η_2 / η_3	2	5	20	100	300	1000	10 000
2	1.40	0.96	1.16	0.74	0.41	0.04	−0.24
5	0.96	1.41	0.86	1.30	0.41	0.17	−0.20
20	1.16	0.86	1.37	1.21	0.60	0.24	−0.06
100	1.07	1.13	1.19	1.37	1.34	0.31	0.13
300	1.29	1.31	1.34	1.36	1.37	1.04	0.19
1000	0.37	0.51	0.77	1.16	1.33	1.36	0.20
10 000	−0.30	−0.27	−0.14	0.04	0.14	0.27	1.27

ters:

$$\begin{aligned}
&x_{\mathbf{size}} = y_{\mathbf{size}} = 1, \quad G_x = 0, \quad G_y = 10,\\
&\eta_1 = 1, \quad \beta_1 = 10^2, \quad \beta_2 = 3 \times 10^3,\\
&c = \eta_1, \quad a = (\eta_3 - \eta_1)/x_{\mathbf{size}}, \quad b = (\eta_2 - \eta_1)/y_{\mathbf{size}},\\
&\rho = \beta_1(ax + by + c) + \beta_2.
\end{aligned}$$

Empty table cells correspond to the case when we have very small errors for all considered grid steps.

2.2 Exponentially varying viscosity

Tables A10–A18 contain log rates of error decreasing with decreasing grid step (the curve slope at Figs. 9 and 12 in logarithmic scale) decreasing for different viscosity contrasts in the case of exponentially varying viscosity. System parameters are the same as in the case of linearly varying viscosity with natural changes:

$$\begin{aligned}
&c = \eta_1, \quad a = (\log \eta_3 - \log \eta_1)/x_{\mathbf{size}}, \quad b = (\log \eta_2 - \log \eta_1)/y_{\mathbf{size}},\\
&\rho = \beta_1 c \exp{(ax + by)} + \beta_2.
\end{aligned}$$

Table 3: Pressure; L_2-error.

η_3 \ η_2	2	5	20	100	300	1000	10 000
2	1.42	1.14	1.24	0.86	0.46	0.08	−0.20
5	1.13	1.44	1.03	1.30	0.57	0.23	−0.16
20	1.23	1.03	1.39	1.27	0.83	0.43	−0.01
100	1.14	1.21	1.26	1.36	1.33	0.50	0.26
300	1.27	1.27	1.29	1.33	1.34	1.17	0.40
1000	0.56	0.70	1.03	1.24	1.31	1.36	0.39
10 000	−0.21	−0.19	−0.04	0.23	0.34	0.43	1.27

Table 4: Velocity v_x; L_∞-error.

η_3 \ η_2	2	5	20	100	300	1000	10 000
2	1.67	1.67	1.41	0.77	0.34	−0.03	−0.30
5	1.63	1.44	1.23	1.04	0.36	0.06	−0.26
20	1.50	1.39	1.11	0.83	0.26	0.09	−0.17
100	0.59	0.79	0.73	1.08	1.43	0.06	−0.04
300	1.59	1.59	1.36	1.36	1.41	0.06	−0.01
1000	−0.29	−0.13	0.29	0.60	1.41	0.03	−0.01
10 000	−0.67	−0.64	−0.51	−0.21	0.07	0.03	0.00

Table 5: Velocity v_x; L_1-error.

η_3 \ η_2	2	5	20	100	300	1000	10 000
2	1.68	2.01	1.91	1.40	0.83	0.40	0.13
5	1.51	1.75	1.96	1.93	1.09	0.60	0.16
20	1.44	1.47	1.70	2.00	1.50	0.99	0.31
100	1.17	1.43	1.56	1.85	2.09	1.39	0.70
300	1.63	1.61	1.63	1.66	1.89	1.87	1.04
1000	0.64	0.84	1.24	1.59	1.61	1.36	1.29
10 000	−0.06	−0.01	0.13	0.53	0.84	1.09	1/12

Table 6: Velocity v_x; L_2-error.

η_3 \ η_2	2	5	20	100	300	1000	10 000
2	1.81	1.99	1.81	1.20	0.70	0.29	0.01
5	1.53	1.61	1.80	1.79	0.91	0.47	0.04
20	1.47	1.54	1.61	1.81	1.09	0.77	0.20
100	1.13	1.39	1.54	1.69	2.04	0.94	0.53
300	1.64	1.63	1.63	1.61	1.70	1.49	0.77
1000	0.56	0.77	1.23	1.57	1.60	1.15	0.90
10 000	−0.19	−0.13	0.01	0.41	0.69	0.96	0.88

Table 7: Velocity v_y; L_∞-error.

η_3 \ η_2	2	5	20	100	300	1000	10 000
2	1.75	1.63	1.47	0.64	0.03	−0.40	−0.67
5	1.67	1.44	1.37	1.23	0.24	−0.26	−0.64
20	1.40	1.23	0.97	0.83	0.34	0.09	−0.51
100	0.83	0.79	0.79	1.33	1.56	0.07	−0.21
300	1.66	1.76	1.91	1.91	1.91	0.66	0.04
1000	−0.01	0.06	0.04	0.37	0.86	1.17	0.03
10 000	−0.30	−0.27	−0.16	−0.06	−0.03	−0.03	−0.30

Table 8: Velocity v_y; L_1-error.

η_3 \ η_2	2	5	20	100	300	1000	10 000
2	1.98	1.51	1.44	1.17	0.59	0.16	−0.13
5	2.01	1.90	1.47	1.63	0.84	0.34	−0.10
20	1.90	1.94	1.94	1.57	1.30	0.73	0.06
100	1.51	1.76	2.00	2.06	1.66	0.81	0.43
300	1.87	1.96	2.04	2.09	2.07	1.44	0.76
1000	0.66	0.86	1.30	1.81	2.07	2.07	0.93
10 000	0.14	0.19	0.34	0.74	1.07	1.34	1.87

Table 9: Velocity v_y; L_2-error.

η_3 \ η_2	2	5	20	100	300	1000	10 000
2	1.99	1.53	1.49	1.14	0.51	0.07	−0.21
5	1.99	1.90	1.54	1.61	0.79	0.26	−0.19
20	1.81	1.80	1.79	1.56	1.24	0.63	−0.03
100	1.27	1.47	1.79	2.03	1.61	0.94	0.34
300	1.86	1.93	1.99	2.04	2.04	1.43	0.60
1000	0.37	0.53	0.90	1.56	1.97	2.03	0.74
10 000	0.019	0.04	0.20	0.54	0.76	0.89	1.23

Table 10: Pressure; L_∞-error.

η_3 \ η_2	2	5	20	100	300	1000	10 000
2	0.94	0.83	0.67	1.01	1.24	1.41	0.84
5	0.87	0.64	0.71	0.84	1.24	1.31	1.16
20	0.73	0.83	0.81	1.01	1.29	1.19	1.04
100	0.80	0.89	1.07	1.30	1.23	1.14	0.96
300	0.90	0.99	1.13	1.23	1.19	1.09	0.91
1000	1.04	1.13	1.14	1.11	1.09	1.03	0.86
10 000	1.19	1.13	0.70	0.91	0.87	0.84	0.71

Table 11: Pressure; L_1-error.

η_3 \ η_2	2	5	20	100	300	1000	10 000
2	1.40	0.89	1.10	1.40	1.46	1.44	1.37
5	0.89	1.13	1.17	1.34	1.41	1.43	1.36
20	0.97	1.14	1.31	1.40	1.40	1.40	1.33
100	1.20	1.36	1.31	1.39	1.39	1.36	1.26
300	1.37	1.36	1.27	1.34	1.36	1.31	1.21
1000	1.39	1.36	1.27	1.29	1.30	1.26	1.17
10 000	1.33	1.29	1.23	1.17	1.14	1.13	1.06

Table 12: Pressure; L_2-error.

η_3 \ η_2	2	5	20	100	300	1000	10 000
2	1.46	1.03	1.20	1.47	1.56	1.53	1.40
5	1.03	1.13	1.23	1.39	1.53	1.51	1.39
20	1.13	1.24	1.31	1.46	1.51	1.46	1.31
100	1.27	1.39	1.39	1.46	1.43	1.37	1.23
300	1.37	1.41	1.39	1.40	1.37	1.31	1.19
1000	1.41	1.41	1.36	1.33	1.30	1.24	1.11
10 000	1.37	1.34	1.26	1.17	1.14	1.11	1.00

Table 13: Velocity v_x; L_∞-error.

η_3 \ η_2	2	5	20	100	300	1000	10 000
2	1.72	1.71	1.61	1.81	1.74	1.70	1.63
5	1.69	1.65	1.41	1.83	1.73	1.66	1.56
20	1.66	1.59	1.36	1.80	1.70	1.56	1.44
100	1.71	1.79	1.90	1.76	1.59	1.46	1.36
300	1.87	2.00	1.89	1.71	1.56	1.46	1.31
1000	1.79	1.87	1.93	1.71	1.54	1.41	1.26
10 000	1.49	1.66	1.91	1.67	1.51	1.37	1.17

Table 14: Velocity v_x; L_1-error.

η_3 \ η_2	2	5	20	100	300	1000	10 000
2	1.89	2.03	2.06	2.17	2.10	2.06	2.01
5	1.61	1.78	2.06	2.24	2.14	2.10	2.01
20	1.59	1.83	2.21	2.21	2.16	2.13	2.04
100	1.64	1.87	2.10	2.21	2.14	2.10	2.04
300	1.76	1.91	2.04	2.21	2.14	2.07	2.01
1000	1.84	1.94	2.04	2.13	2.14	2.06	1.97
10 000	1.77	1.87	1.96	2.00	2.01	2.00	1.91

Table 15: Velocity v_x; L_2-error.

η_3 \ η_2	2	5	20	100	300	1000	10 000
2	1.92	2.00	1.97	2.03	2.00	1.96	1.91
5	1.66	1.82	1.93	2.09	2.01	1.97	1.90
20	1.63	1.84	2.06	2.09	2.01	1.96	1.87
100	1.71	1.93	2.06	2.04	1.97	1.90	1.83
300	1.87	1.99	2.03	2.00	1.93	1.84	1.74
1000	1.93	2.00	2.03	2.00	1.93	1.84	1.74
10 000	1.76	1.89	1.96	1.94	1.90	1.83	1.67

Table 16: Velocity v_y; L_∞-error.

η_3 \ η_2	2	5	20	100	300	1000	10 000
2	1.76	1.67	1.83	1.87	1.71	1.71	1.56
5	1.73	1.56	1.53	2.09	1.99	1.90	1.89
20	1.67	1.46	1.37	1.96	1.89	1.86	1.84
100	1.57	1.27	1.80	1.77	1.69	1.64	1.61
300	1.27	1.80	1.79	1.67	1.57	1.53	1.50
1000	1.81	1.81	1.73	1.56	1.49	1.43	1.36
10 000	1.71	1.16	1.56	1.40	1.36	1.29	1.19

Table 17: Velocity v_y; L_1-error.

η_3 \ η_2	2	5	20	100	300	1000	10 000
2	1.91	1.63	1.74	2.16	2.13	2.11	2.03
5	2.03	1.91	1.97	2.13	2.17	2.19	2.14
20	2.03	2.01	2.26	2.21	2.20	2.20	2.14
100	2.01	2.24	2.29	2.31	2.30	2.26	2.17
300	2.26	2.34	2.27	2.23	2.26	2.26	2.17
1000	2.24	2.24	2.23	2.17	2.17	2.17	2.16
10 000	2.07	2.10	2.11	2.11	2.09	2.07	2.07

Table 18: Velocity v_y; L_2-error.

η_3 \ η_2	2	5	20	100	300	1000	10 000
2	1.97	1.66	1.81	2.10	2.01	1.94	1.83
5	2.00	1.93	1.99	2.11	2.10	2.04	1.94
20	1.97	1.90	2.09	2.14	2.11	2.07	2.00
100	1.89	1.96	2.11	2.09	2.06	2.04	1.97
300	2.03	2.11	2.09	2.01	1.97	1.96	1.93
1000	2.11	2.06	2.04	1.96	1.91	1.87	1.86
10 000	1.96	1.94	1.93	1.87	1.83	1.77	1.71